Electronic Supplementary Material (ESI) for Journal of Materials Chemistry A.
This journal is © The Royal Society of Chemistry 2019

Electronic supplementary information (ESI)

Electroreduction of CO_2 to formate on amine modified Pb electrodes

Nidhal Zouaoui[a], Benjamin D. Ossonon[a], Mengyang Fan[a], Dilungane Mayilukila[a], Sebastien Garbarino[a], Glynis de Silveira[b], Gianluigi A. Botton[b], Daniel Guay[a], Ana C. Tavares[a,*]

[a] Institut National de la Recherche Scientifique – Énergie, Matériaux et Télécommunications, 1650 Boulevard Lionel-Boulet, Varennes (Qc), Canada, J3X 1S2

[b] Department of Materials Science and Engineering, McMaster University, 1280 Main Street West, Hamilton (On), Canada, L9H 4L7

***Corresponding author :** Ana C. Tavares, ana.tavares@emt.inrs.ca

Table S1. Comparison of $FE_{formate}$ on different Pb-based electrodes and PEI-NCNT[(a)] electrode

Catalysts	Electrolyte	Electrolysis potential (V vs. RHE)	Current density (mA cm^{-2})	$FE_{formate}$ (%)	Reference
Pb	0.5 M $KHCO_3$	-1.17	-5.5	~72	[1]
Pb granules	0.5 M $KHCO_3$	-1.03	-1.13	74	[2]
Pb plate	0.5 M NaOH	-0.86	-2.5	65	[3]
Oxide-derived Pb	0.5 M $NaHCO_3$	-0.8	-0.6	98	[4]
Electrochemically roughened Pb	0.1 M $KHCO_3$	-0.96	-1.17[(b)]	88	[5]
Porous Pb (100)	1 M $KHCO_3$	-0.99	-8.0	97	[6]
PEI-NCNT[(a)]	0.1 M $KHCO_3$	-1.15[(c)]	-9.5	87	[7]
Amine-derived Pb	1 M $KHCO_3$	-1.09	-9.5	94	This work

[(a)] Polyethyleneamine adsorbed on the surface of nitrogen-doped carbon nanotubes.

[(b)] Partial current density for formate.

[(c)] A pH value of 6.8 (measured experimentally in a 0.1 M $KHCO_3$ solution saturated with CO_2) was used to convert the potential value -1.8 V vs SCE reported in [7] to the RHE scale.

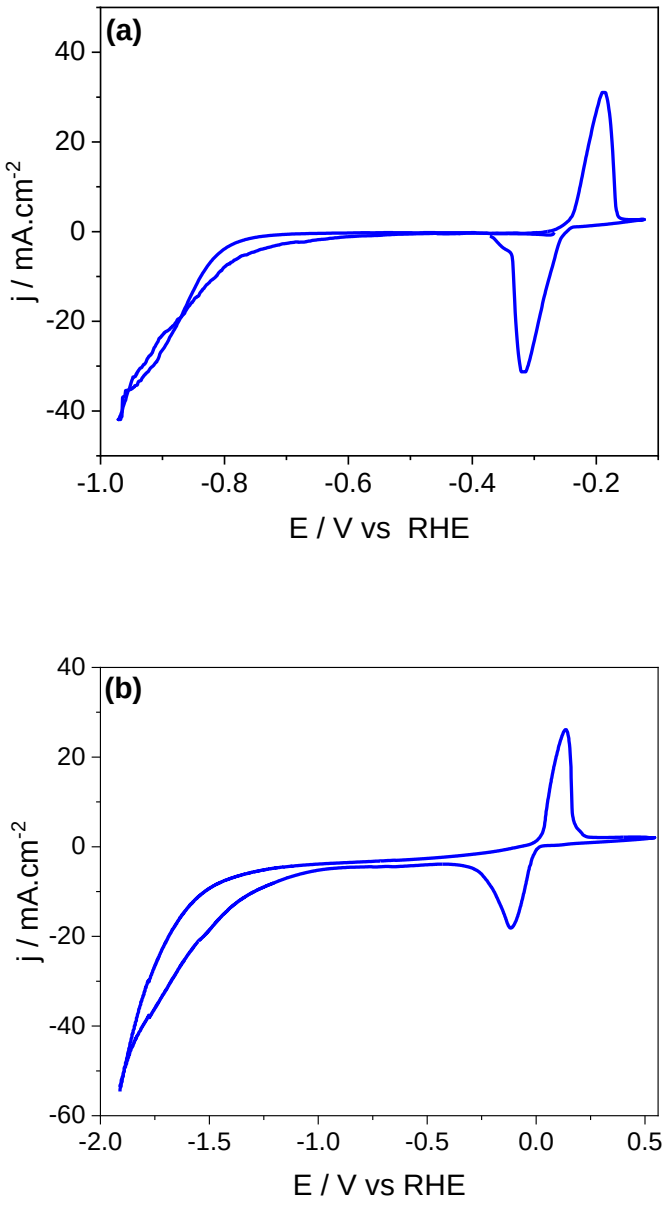

Fig. S1. Cyclic voltammograms of bare Pb electrodes in **(a)** N_2-saturated 0.5 M HCl and **(b)** N_2-saturated 1 M $KHCO_3$ recorded at a scan rate of 10 $mV \cdot s^{-1}$.

The cyclic voltammogram illustrates the oxidation and reduction processes occurring at a Pb electrode immersed in the two electrolytes. In Fig. S1.a the anodic peak corresponds to the oxidation of Pb to $PbCl_2$, and the cathodic peak to the reduction of $PbCl_2$ to Pb [8]. In Fig. S1.b, the anodic and cathodic peaks are attributed to the oxidation metallic Pb to $Pb(OH)_2$ / PbO and their reduction to Pb [9,10].

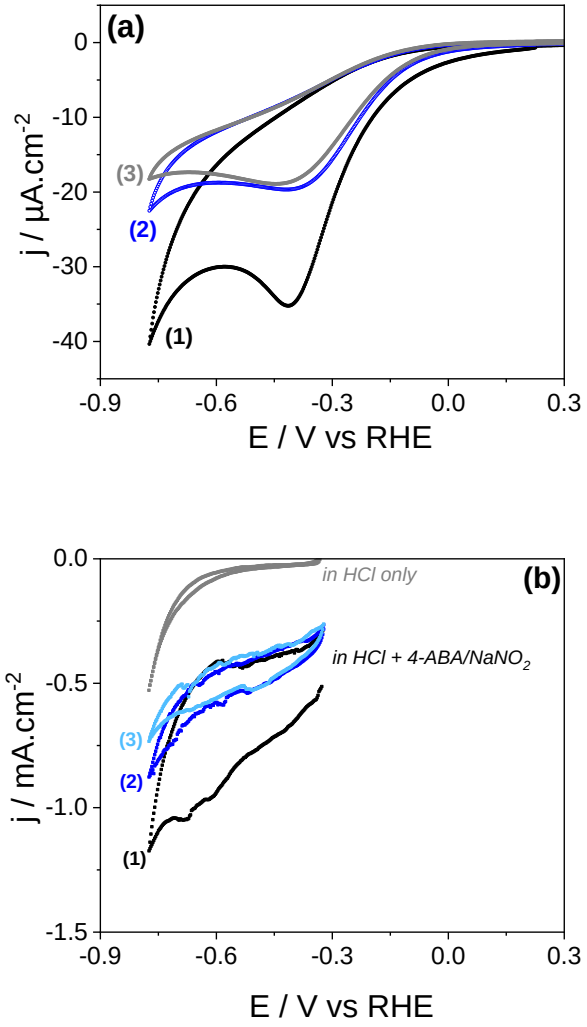

Fig. S2. Cyclic voltammograms of **(a)** glassy carbon electrode and **(b)** Pb electrode in N_2-saturated 0.5 M HCl, 2 mM 4-aminobenzylamine (4-ABA) and 2 mM $NaNO_2$ recorded at 10 $mV \cdot s^{-1}$. The cycle number is indicated next to the voltammograms.

The cathodic peak related to the reduction and grafting of the 4-aminobenzyldiazonium cation at the surface of the working electrode is observed at -0.45 V vs RHE for the glassy carbon electrode. On Pb, reduction and grafting of the 4-aminobenzyldiazonium cation results in a large current increase between -0.4 and -0.6 V

vs RHE. In both cases, the current decreases between the first and second cycle indicating the formation of an organic layer on the electrodes` surface [11, 12]. However, the current density does not decrease significantly from the second to the third cycle. This indicates that the film is conductive or does not cover the entire surface of the electrode, further allowing the reduction of the diazonium cations and the formation of radicals [12].

The current density on the Pb electrode is significantly higher compared with the one recorded with the glassy carbon electrode. This can be explained by the different reactivity of the two materials. The open circuit voltage of Pb electrode in the HCl electrolyte (-0.07 V vs RHE) shows that this material is easily oxidized (see Figure S1). As demonstrated elsewhere, the grafting of diazonium cations is favored on metals that are easily oxidized [13].

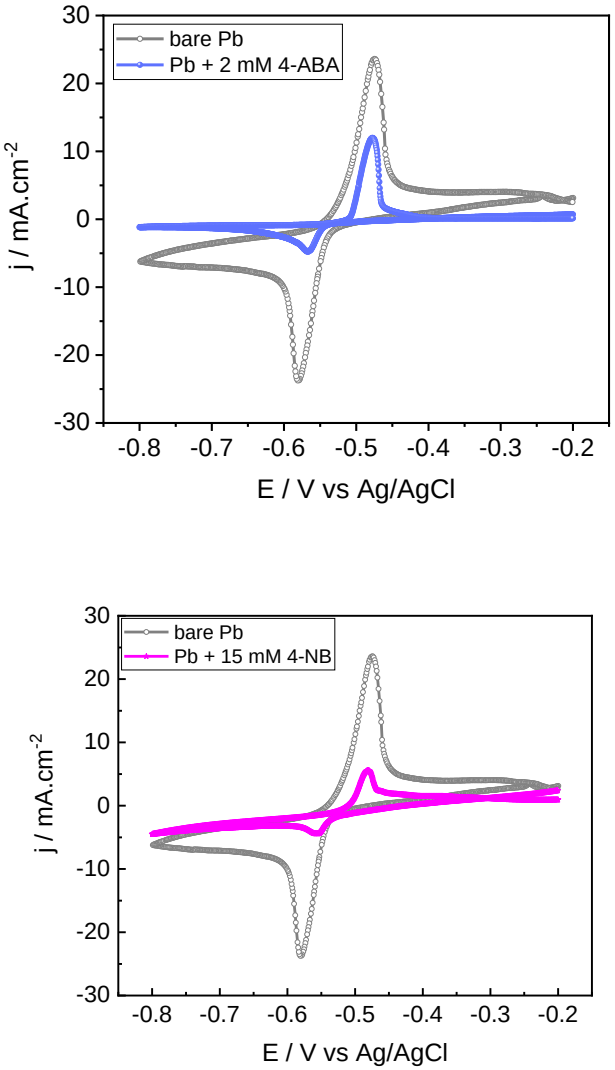

Fig. S3. Example of cyclic voltammograms (first cycle) recorded at 5 mVs^{-1} in 0.5 M H_2SO_4 and used to determine the electrochemical surface area of the Pb and Pb- modified electrodes with 4-ABA (2 mM) and 4-NB (15 mM).

The charge under the anodic peak, which corresponds to the oxidation of Pb to $PbSO_4$, was used to calculate the Pb_{ESCA} using the following relation Pb_{ESCA} (cm^2) = Q_{an} (mC)/ 300 μCcm^{-2}, where 300 μCcm^{-2} is the calculated specific charge density of polycrystalline

metallic lead, assuming a 2 e^- process and an equal repartition of (111), (110) and (100) surface orientations [14].

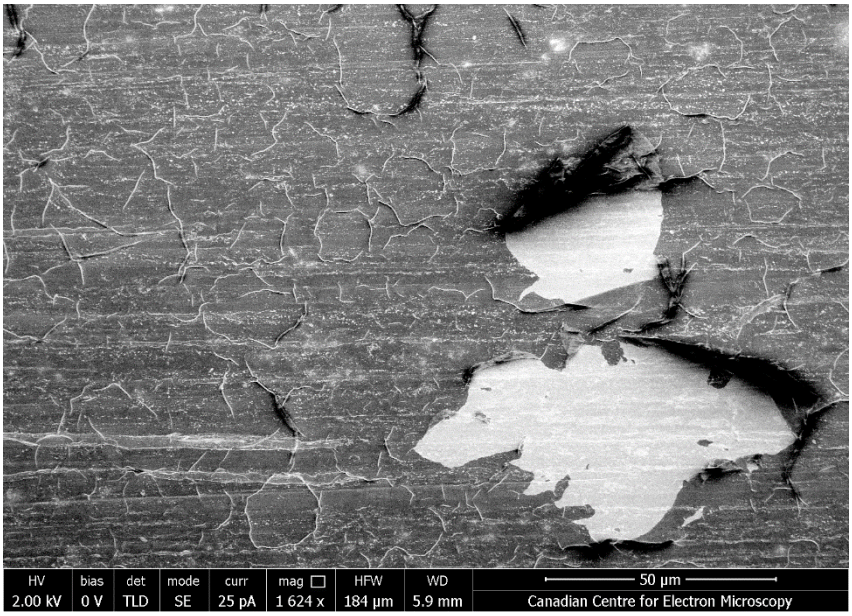

Fig. S4. Scanning electron microscopy of a 4-ABA polymer film grown on Pb substrate using [4-ABA] = 10 mM. The extent of grafting is $\tau = 16 \times 10^{-7}$ mol·cm^{-2}.

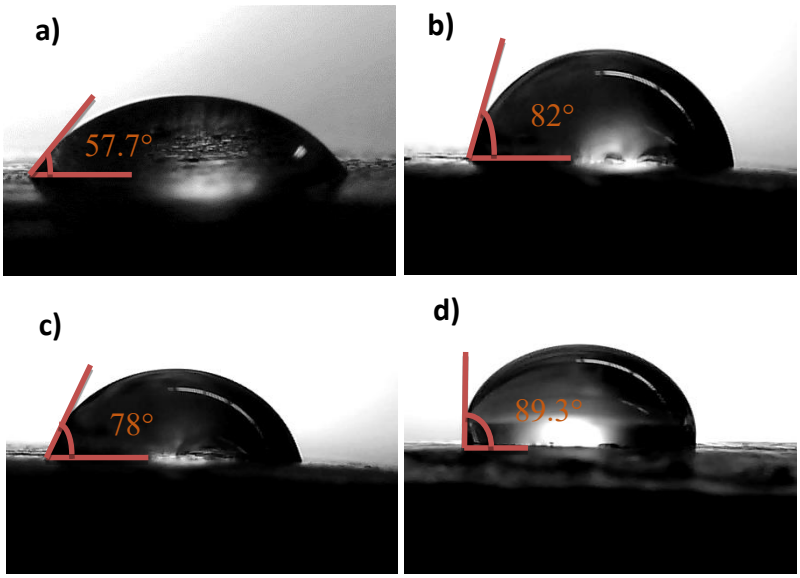

Fig. S5. Water contact angle on **(a)** bare Pb electrode and Pb-modified electrodes with **(b)** 4-aminobenzyldiazonium (4-ABA, $\tau = 6.3 \times 10^{-7}$ mol·cm^{-2}), **(c)** 3-aminobenzyldiazonium (3-ABA; $\tau = 2.3 \times 10^{-7}$ mol·cm^{-2}), and **(d)** 4-(2-aminoethyl)benzenediazonium (AEA; $\tau = 7.2 \times 10^{-7}$ mol·cm^{-2}).

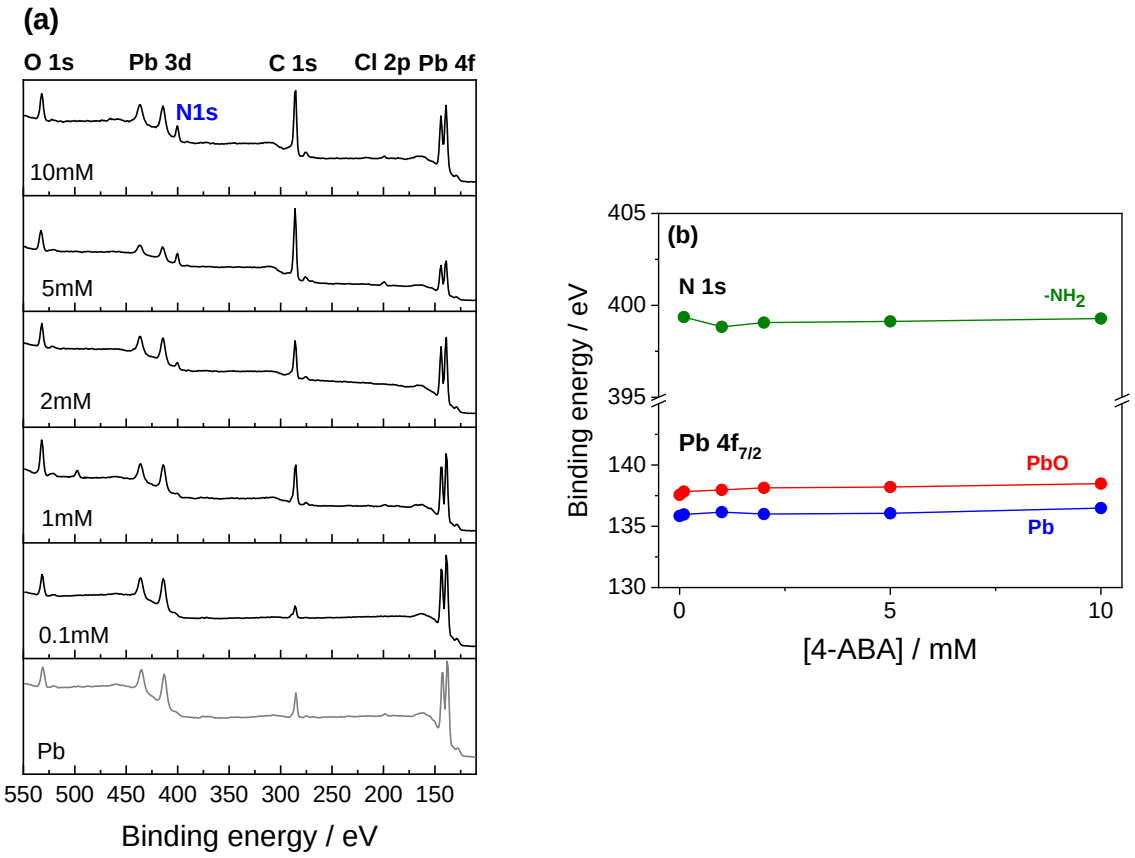

Fig. S6. (a) XPS survey spectra of bare Pb and Pb + 4-ABA surfaces. The concentrations of 4-aminobenzylamine (4-ABA) in the grafting solution are indicated in the spectra; **(b)** Variation of the binding energy values of the peaks in the high resolution Pb $4f_{7/2}$ and N 1s spectra as a function of the amine concentration.

The surface functionalization of the Pb electrodes with the amine polyarylene layer was confirmed by XPS, **Fig. S5**. The peaks characteristic of C, N, O, Pb and Cl are present in the spectra of the Pb + 4-ABA electrodes. The intensity of the C 1s and N 1s peaks increases with the concentration of 4-ABA in the grafting solution. The Cl (less than 3 at%)

comes from the electrolyte (HCl) used for reduction of the Pb surface and grafting of the polyarylene layers.

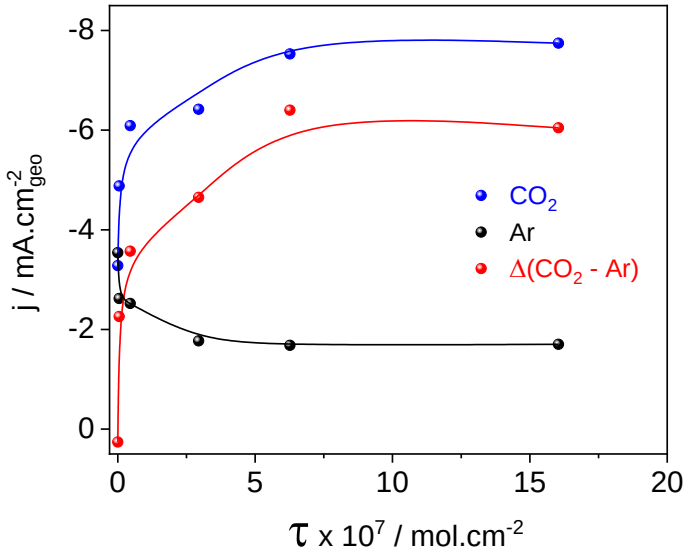

Fig. S7. Variation of the current density recorded at -1.09 V vs RHE in Ar-saturated and CO_2-satuared 1 M $KHCO_3$ electrolyte as a function of the extent of grafting.

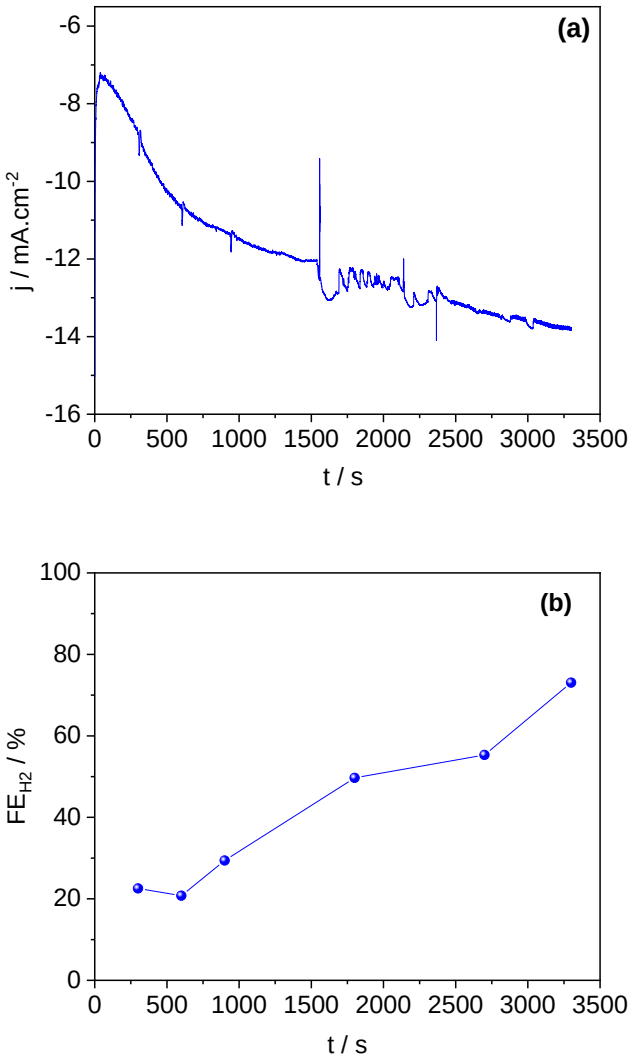

Fig. S8. (a) Chronoamperogram (1h) recorded with Pb bare electrode in CO_2-saturated 1 M $KHCO_3$ and (b) Variation of the Faradic efficiency for H_2.

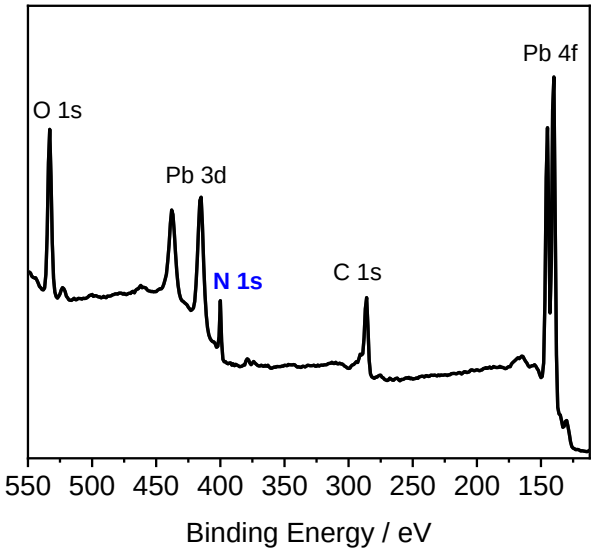

Fig. S9. XPS survey spectrum of Pb + 4-ABA (τ= 6.3 × 10^{-7} mol·cm^{-2}) after 11 h electrolysis in CO_2-saturated 1M $KHCO_3$ electrode.

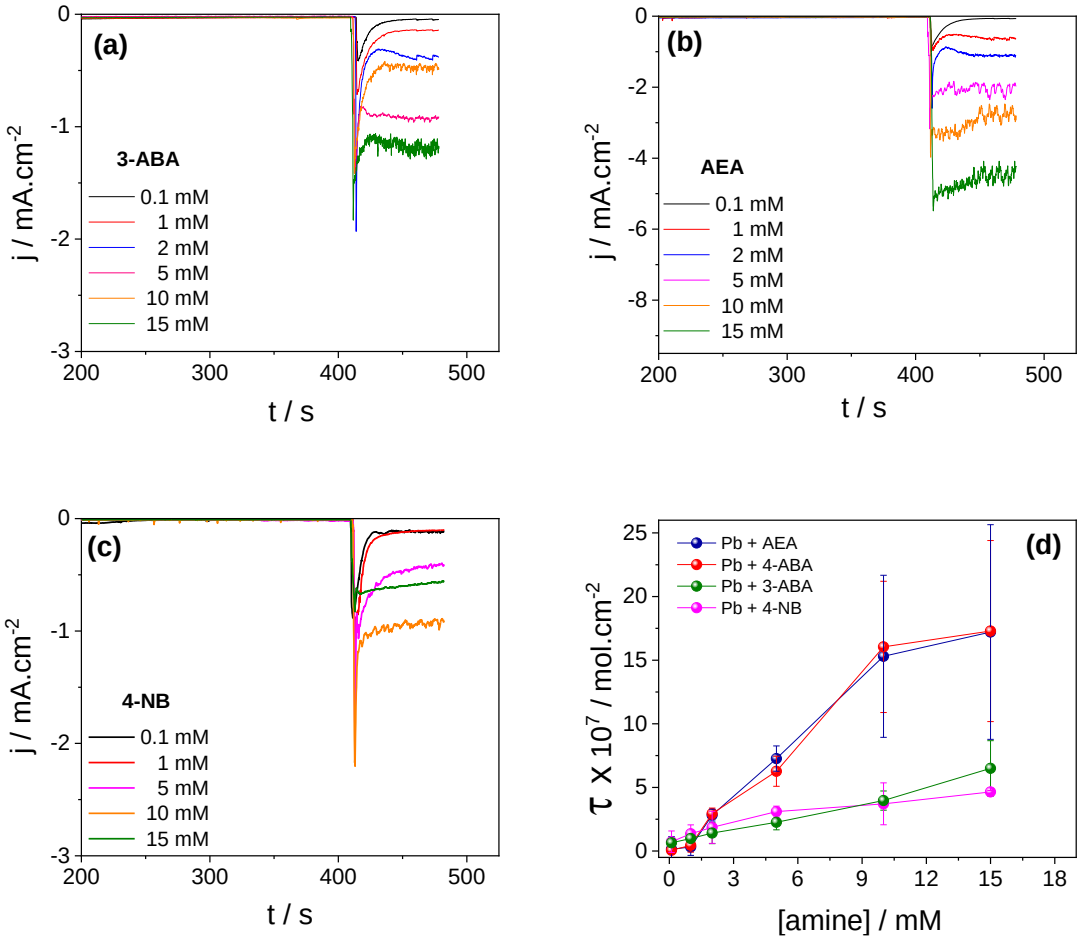

Fig. S10. Chronoamperograms recorded during the electrografting of **(a)** 3-aminobenzyldiazonium (3-ABA), **(b)** 4-(2-aminoethyl)benzenediazonium (AEA), **(c)** 4-nitrophenyldiazonium (4-NB) on the surface of Pb electrodes in 0.5 M HCl. The potential is kept at -0.52 V vs RHE for 7 mins to reduce the Pb's surface to its metallic form; after which the solution containing the amine / $NaNO_2$ (1:1 molar ratio) is injected in the electrochemical cell and the grafting reaction allowed proceeding for 60 s; **(d)** Variation of the extent of grafting (τ) with the concentration of the amines in the grafting solution. Data for 4-aminomethyldiazonium (4-ABA) is included in figure (d) for comparison. At least

three grafting experiments were done for each amine concentration and the error bars correspond to the standard deviation for each data set.

As illustrated in **Fig. S10d**, τ increases linearly with the amine concentration in the solution. Similar τ values were found for 4-ABA and AEA, which was expected considering that these two amines are structurally similar, thus their diazonium cations should have identical reactivity [12]. Instead, 3-ABA has the phenyl amine group in *meta* position, and blocking of this position generally slows down the grafting reaction [15]. For 4-NB, the NO_2 group decreases the electronic density of the aromatic ring, deactivating it for the electrophylic attack by the nitrosyl cation [16], thus lowering the grafting rate.

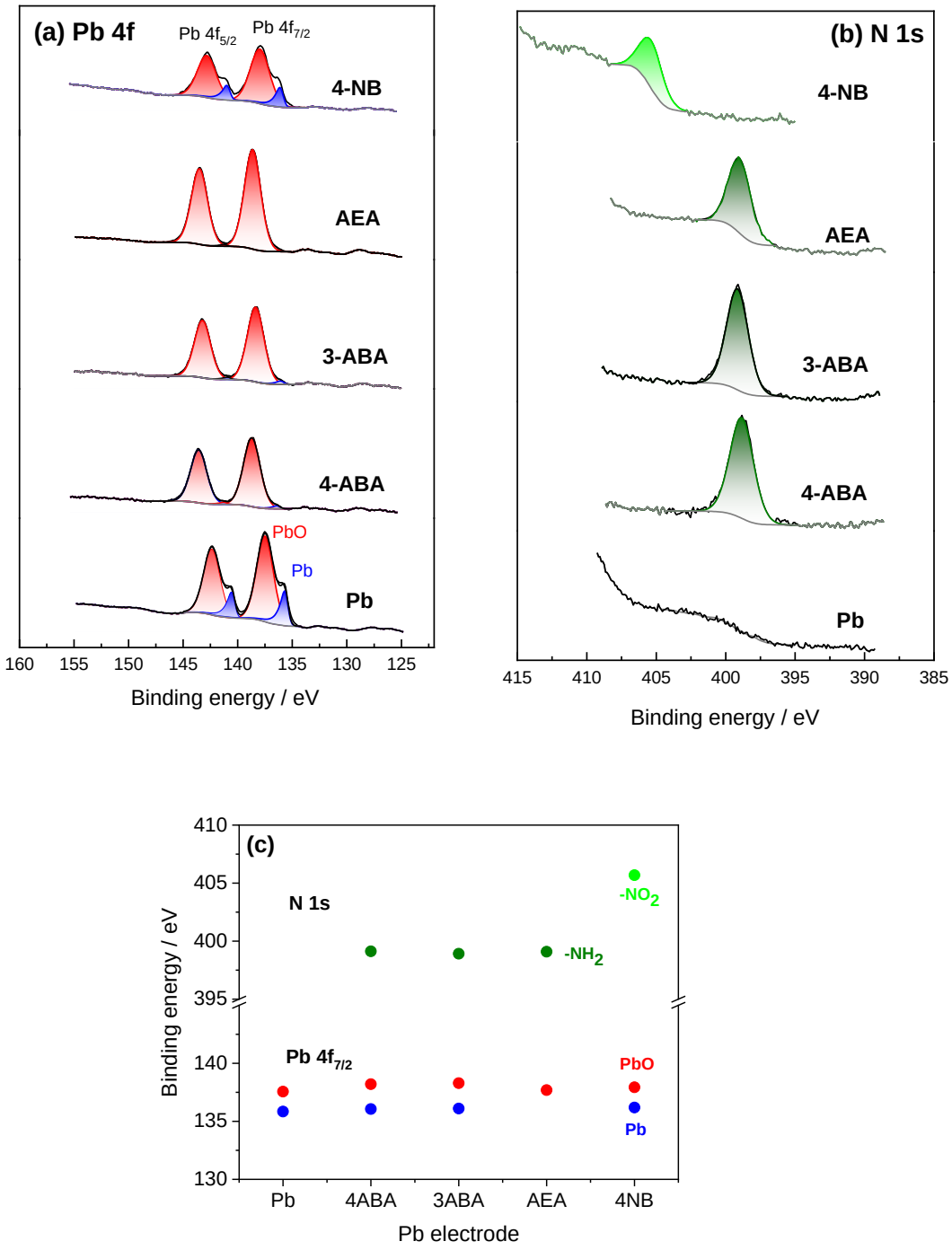

Fig. S11. XPS core level spectra **(a)** Pb 4f and **(b)** N 1s of the bare Pb electrode and Pb electrodes modified with 4-aminobenzyldiazonium (4-ABA, $\tau = 6.3 \times 10^{-7}$ mol·cm^{-2}), 4-(2-aminoethyl)benzenediazonium (AEA, $\tau = 7.2 \times 10^{-7}$ mol·cm^{-2}), 3-

aminobenzyldiazonium (3-ABA, $\tau = 6.5 \times 10^{-7}$ mol·cm^{-2}) and nitrophenyldiazonium (4-NB, $\tau = 4.6 \times 10^{-7}$ mol·cm^{-2}); **(c)** Variation of the binding energy values of the peaks in the high resolution Pb $4f_{7/2}$ and N 1s spectra as a function of the type of amine.

The high resolution Pb 4f and N 1s spectra of the Pb modified electrodes with the four diazonium salts are presented in **Fig. S11a** and **Fig. S11b**, respectively. The Pb 4f spectra of Pb, Pb+4-ABA, Pb+3-ABA and Pb+4-NB contain a pair of peaks centered at ~ 138 and ~ 143 eV attributed to oxidized Pb [17], and a second pair of peaks centered at ~ 136 and ~ 141 eV associated to Pb^0 [17, 18]. The spectrum of Pb-AEA contains only the peaks associated to PbO. A single peak at ~ 399 eV and attributed to the NH_2 functional group is found in the high resolution N 1s spectra of Pb+4-ABA, Pb+3-ABA and Pb-AEA. In the case of Pb+4-NB, the single peak at ~ 405.7 eV is attributed to the NO_2 functional group [19].

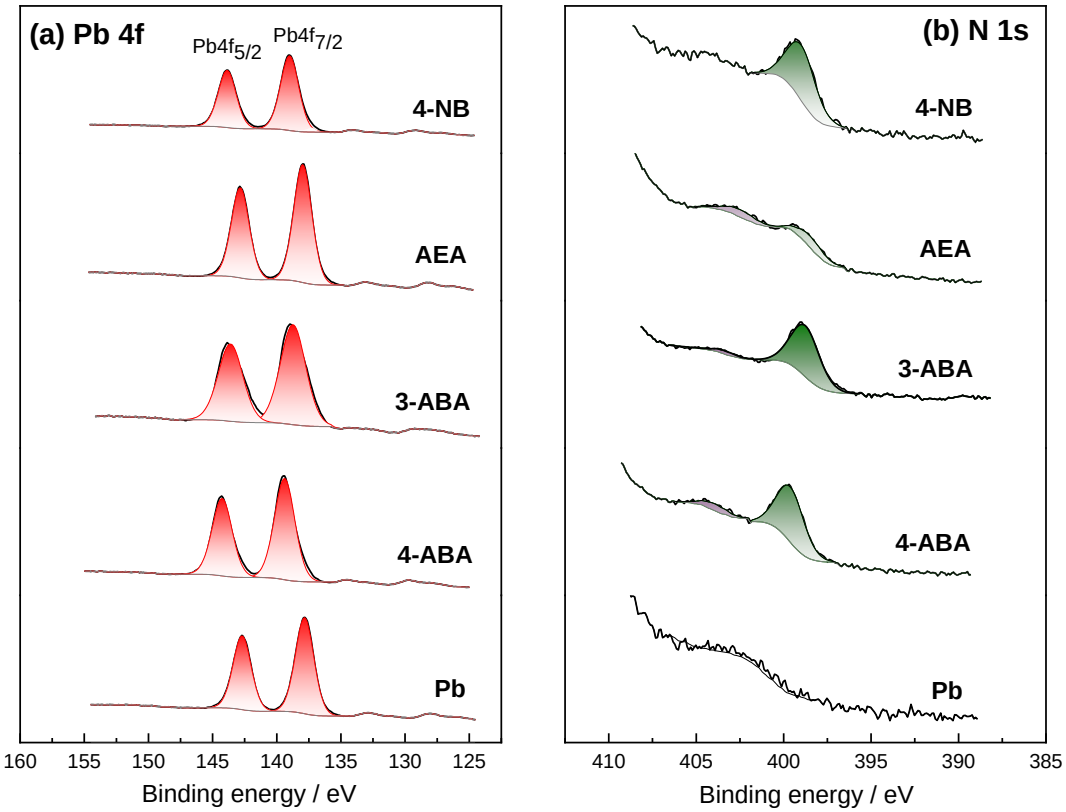

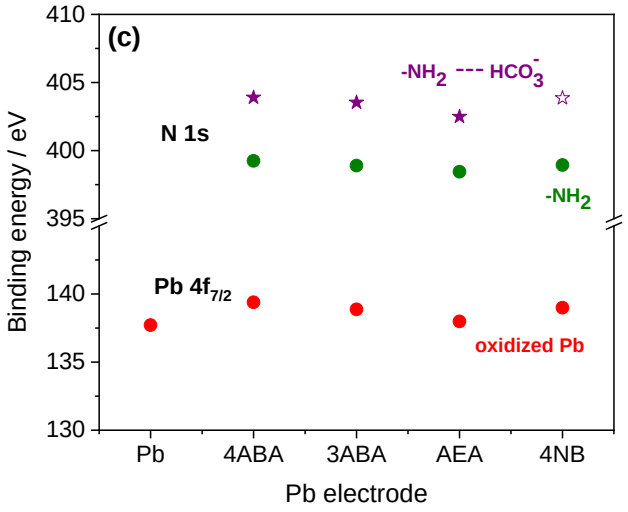

Fig. S12. XPS core level spectra **(a)** Pb 4f and **(b)** N 1s after electroreduction of CO_2 for the bare Pb electrode and Pb electrodes modified with 4-ABA ($\tau = 6.3 \times 10^{-7}$ mol·cm^{-2}),

AEA ($\tau = 7.2 \times 10^{-7}$ mol·cm^{-2}), 3-ABA ($\tau = 6.5 \times 10^{-7}$ mol·cm^{-2}) and 4-NB ($\tau = 4.6 \times 10^{-7}$ mol·cm^{-2}); **(c)** Variation of the binding energy values of the peaks in the high resolution Pb $4f_{7/2}$ and N 1s spectra as a function of the type of amine.

The high resolution Pb 4f and N 1s spectra of the Pb modified electrodes after electrolysis are presented in **Fig. S12a** and **Fig. S12b**, respectively. The Pb 4f spectra are still dominated by the features attributed to the oxidized Pb, with no spectral lines associated to Pb^0. A peak at ~ 399 eV and attributed to the NH_2 functional group is found in the high resolution N 1s spectra of all samples. In the case of 4-NB, this shows that the $–NO_2$ group initially present on the surface of the Pb modified electrode was reduced to $–NH_2$ during the electrolysis. The N 1s spectra contain a second peak at higher binding energy **(**~ 403 eV) which could result from the interaction between the protonated amine and the hydrogen carbonate anions [20]. **Fig. S12b** also shows that the amount of NH_2 groups decreased significantly for Pb + AEA electrode. This probably results from the nucleophilic attack of OH^- group on the aliphatic H in β position, leading to the loss of NH_2 groups [21].

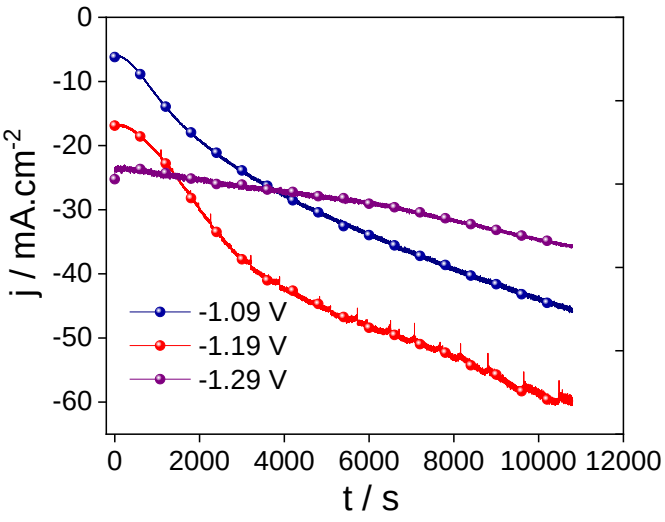

Fig. S13. Chronoamperograms recorded with Pb bare electrode in CO_2-saturated 1 M $KHCO_3$.

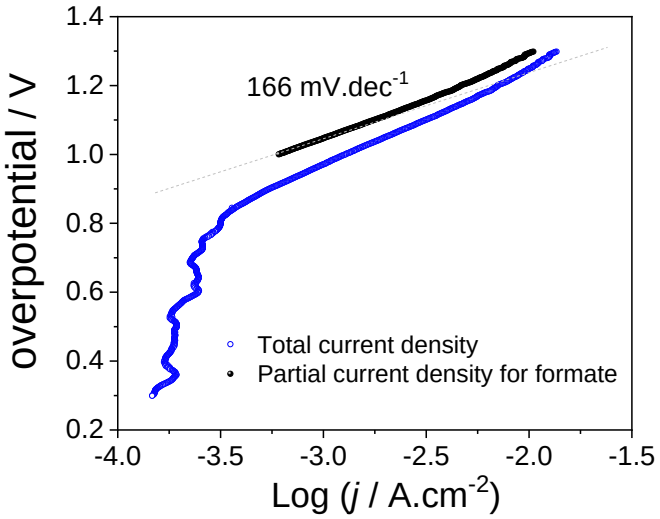

Fig. S14. Tafel analysis of a polarization curve recorded at 5 $mV \cdot s^{-1}$ for bare Pb electrode in CO_2-saturated 1 M $HKCO_3$ electrolyte.

References

1. K. K. Yoshio Hori, Shin Suzuki, *Chemistry Letters*, 1985, **11**, 1695-1698.
2. F. Koleli, T. Atilan, N. Palamut, A. M. Gizir, R. Aydin and C. H. Hamann, *J. Appl. Electrochem.* , 2003, **33**, 447–450.
3. B. Innocent, D. Liaigre, D. Pasquier, F. Ropital, J. M. Léger and K. B. Kokoh, *J. Appl. Electrochem.* , 2009, **39**, 227-232.
4. C. H. Lee and M. W. Kanan, *ACS Catal.*, 2015, **5**, 465-469.
5. Z. He, J. Shen, Z. Ni, J. Tang, S. Song, J. Chen and L. Zhao, *Catalysis Communications*, 2015, **72**, 38-42.
6. M. Fan, S. Garbarino, G. A. Botton, A. C. Tavares and D. Guay, *Journal of Materials Chemistry A*, 2017, **5**, 20747-20756.
7. S. Zhang, P. Kang, S. Ubnoske, M. K. Brennaman, N. Song, R. L. House, J. T. Glass and T. J. Meyer, *Journal of the American Chemical Society*, 2014, **136**, 7845-7848.
8. R. G. Barradas, K. Belinko and J. Ambrose, *Canadian Journal of Chemistry*, 1975, **53**, 389-406.
9. V. I. Birss and M. T. Shevalier, *Journal of The Electrochemical Society*, 1987, **134**, 1594-1600.
10. A. S. Kumawat and A. Sarkar, *Journal of The Electrochemical Society*, 2017, **164**, H1112-H1120.
11. S. Baranton and D. Bélanger, *The Journal of Physical Chemistry B*, 2005, **109**, 24401-24410.
12. T. Breton and D. Bélanger, *Langmuir*, 2008, **24**, 8711-8718.
13. A. Adenier, E. Cabet-Deliry, A. Chaussé, S. Griveau, F. Mercier, J. Pinson and C. Vautrin-Ul, *Chemistry of Materials*, 2005, **17**, 491-501.
14. Y. Liu, S. Bliznakov and N. Dimitrov, *The Journal of Physical Chemistry C*, 2009, **113**, 12362-12372.
15. C. Combellas, D.-e. Jiang, F. Kanoufi, J. Pinson and F. I. Podvorica, *Langmuir*, 2009, **25**, 286-293.
16. D. Belanger and J. Pinson, *Chemical Society Reviews*, 2011, **40**, 3995-4048.
17. S. Rondon and P. M. A. Sherwood, *Surface Science Spectra*, 1998, **5**, 97-103.
18. NIST X-ray Photoelectron Spectroscopy Database, Version 4.1 (web version, http://srdata.nist.gov/xps/), http://srdata.nist.gov/xps/.).
19. B. Ortiz, C. Saby, G. Y. Champagne and D. Bélanger, *Journal of Electroanalytical Chemistry*, 1998, **455**, 75-81.
20. S. Stegmeier, M. Fleischer, A. Tawil, P. Hauptmann, K. Egly and K. Rose, *Procedia Chemistry*, 2009, **1**, 236-239.
21. A. A. Zagorodni, D. L. Kotova and V. F. Selemenev, *Reactive and Functional Polymers*, 2002, **53**, 157-171.